https://rbgeomorfologia.org.br/
ISSN 2236-5664

Revista Brasileira de Geomorfologia

v. 27, nº 4 (2026)

http://dx.doi.org/10.20502/rbg.v27i4.2782

Research paper

Impact of Vegetation on Hydrosedimentological Connectivity in the Tigre Creek Basin, Semi-Arid Region of Paraíba

Impacto da Vegetação na Conectividade Hidrossedimentológica da Bacia do Tigre Creek, Semiárido Paraibano

Adonai Felipe Pereira de Lima Silva [1], Jonas Otaviano Praça de Souza [2]

[1] Federal University of Paraíba, Semi-Arid Fluvial Environments Study Group (GEAFS), João Pessoa, Paraíba, Brazil. E-mail: ad.felipelima@hotmail.com
ORCID: https://orcid.org/0000-0002-1654-6775

[2] Federal University of Paraíba, Center for Exact and Natural Sciences, Department of Geosciences, João Pessoa, Paraíba, Brazil. E-mail: jonas.souza@academico.ufpb.br
ORCID: https://orcid.org/0000-0002-1405-0944

Received: 27/01/2026; Accepted: 31/08/2026; Published: 17/11/2026.

Abstract: Hydrosedimentological connectivity is a key concept for understanding the transfer of water and sediment within drainage basins, particularly in semi-arid environments characterized by strong climatic seasonality. This study aims to evaluate the influence of vegetation on hydrosedimentological connectivity in the Tigre Creek Basin, located in the semi-arid region of Paraíba State, Brazil, while accounting for seasonal variations in biomass. A total of 51 Landsat images (2014–2023) were used to calculate the NDVI, associated with 90- and 120-day antecedent accumulated rainfall (AAR), derived from pluviometric data provided by the Executive Agency for Water Management of the State of Paraíba (AESA) and the Pernambuco Agency for Water and Climate (APAC). Based on these data, four vegetation scenarios (very dry, dry, medium and wet) were defined, and the Connectivity Index (CI) was applied. The results indicate higher connectivity under low biomass conditions and a progressive reduction in connectivity as vegetation density increases. These findings demonstrate that vegetation plays a fundamental role in controlling hydrosedimentological connectivity and highlight the importance of seasonal approaches for understanding erosion processes and supporting environmental planning in semi-arid river basins.

Keywords: Dryland fluvial systems; Rainfall and vegetation seasonality; Sediment transfer.

Resumo: A conectividade hidrossedimentológica representa um elemento central para a compreensão da transmissão de fluxos de água e sedimentos em bacias hidrográficas, especialmente em ambientes semiáridos marcados por elevada sazonalidade climática. Este estudo tem como objetivo avaliar a influência da vegetação na conectividade hidrossedimentológica da Bacia do Tigre Creek, localizada no semiárido paraibano, considerando diferentes cenários sazonais de biomassa. Para isso, foram utilizadas 51 imagens Landsat (2014–2023) para o cálculo do NDVI, associado à precipitação antecedente acumulada (CAA) de 90 e 120 dias, obtida a partir de dados pluviométricos da Agência Executiva de Gestão das Águas do Estado da Paraíba (AESA) e Agência Pernambucana de Águas e Clima (APAC). Com base nesses dados, foram definidos quatro cenários de vegetação (muito seco, seco, médio e úmido), aos quais foi aplicado o Índice de Conectividade (IC). Os resultados indicam maior conectividade nos cenários com menor densidade de biomassa e redução progressiva da conectividade com o aumento da cobertura vegetal. Conclui-se que a vegetação exerce papel fundamental na modulação da conectividade hidrossedimentológica, reforçando a importância de abordagens sazonais para o entendimento dos processos erosivos e o planejamento ambiental em bacias semiáridas.

Palavras-chave: Sistemas fluviais de Terras Secas; Sazonalidade da chuva e da vegetação; Transferência de sedimentos.

1. Introduction

The process of flow transmission in river basins can be influenced by natural or anthropogenic factors that interfere with the circulation of matter and energy, requiring specific studies of their impacts at different spatiotemporal scales (ALMEIDA; CORREA, 2020). This complexity makes geomorphological processes dynamic and susceptible to problems such as sedimentation of rivers and reservoirs, contamination, and the impairment of water use for supply and irrigation (PEREIRA, 2025; SCAPIN; PAIVA; BELING, 2007).

The analysis of flow transmission in river basins is largely grounded in the concept of landscape connectivity, which represents the capacity for interaction and circulation of matter and energy among environmental compartments (BRIERLEY; FRYIRS; JAIN, 2006; SOUZA; CORREA, 2012; BLANTON; MARCUS, 2013; FRYIRS, 2013; WOHL, 2017). This connectivity can occur across different dimensions—vertical, lateral, and longitudinal—and is expressed through both hydrological and sedimentological processes (BRACKEN; CROKE, 2007; BLANTON; MARCUS, 2013; BRACKEN et al., 2013).

Sediment connectivity is associated with the physical and functional linkage that controls the transport and storage of particles between source areas and downstream regions of a river basin (MARCHAMALO; HOOKE; SANDERCOCK, 2016; CAVALLI et al., 2013; WOHL, 2017; JAMES, 2018; NAJAFI et al., 2021). Complementarily, hydrological connectivity describes the capacity of water to mediate the transport of matter, energy, and organisms, contributing to the understanding of surface and subsurface flow behaviour (PRINGLE, 2003; BRACKEN et al., 2013; POEPPL; KEESSTRA; MAROULIS, 2017).

The intensity of erosional processes depends on factors such as flow regime, vegetation, soil, and climate. In semiarid environments with low infiltration capacity and sparse vegetation cover, runoff-driven erosion processes predominate, favoured by intense rainfall and shallow soils, resulting in high rates of sediment transport (MICHAELIDES; MARTIN, 2012; BRACKEN; WAINWRIGHT, 2008; SILVA JR et al., 2011; HENARES; DONSELAAR; CARACCIOLO, 2020). In addition, geology and soil permeability influence hydrological flow pathways: areas with permeable soils increase subsurface flows, whereas impermeable soils intensify surface runoff (LEIBOWITZ et al., 2018).

Vegetation, in turn, plays a fundamental role in reducing hydrological and sedimentological connectivity by acting as a barrier to surface runoff, particularly during extreme events (SANDERCOCK; HOOKE; MANT, 2007; LESSCHEN; SCHOORL; CAMMERAAT, 2009). The relationship between vegetation cover, morphology, and fluvial processes in arid and semiarid regions reveals that Dryland channels exhibit high morphological complexity and irregularity, influenced by variations in riparian vegetation along the channel (SANDERCOCK; HOOKE; MANT, 2007; MILAN et al., 2018). In these areas, intermittent surface flow in ephemeral rivers creates specific habitats and plays a fundamental role in dryland ecosystems, although their hydrological interactions and riparian forest structure remain poorly understood (MORGAN et al., 2020).

In river basins with intensive agricultural activity, vegetation removal and increased hillslope erosion intensify sediment transport, causing sediment deposition in valleys and even channel disappearance (FARIA, 2014; LIMA; FELTRIN, 2019). Limited vegetation cover, combined with the dominance of Hortonian overland flow, makes bedload sediment transport a recurrent process in several arid and semiarid regions worldwide (TOOTH, 2000).

At the hillslope scale, microtopography and the spatial distribution of vegetation—composed of mosaics of vegetated patches and exposed soil—control hydrological connectivity, resulting in discontinuous and irregular runoff (LESSCHEN; SCHOORL; CAMMERAAT, 2009). Thus, vegetation is an essential factor in reducing sediment connectivity, helping mitigate erosion, desertification, and land degradation (SANDERCOCK; HOOKE; MANT, 2007).

The importance of this study in the Tigre Creek Basin is justified by its location in the headwaters of the Paraíba River, the main fluvial system in the state of Paraíba, and by the hydroclimatic characteristics typical of the Cariri region of Paraíba, one of the driest regions in Brazil. The combination of highly seasonal rainfall, predominantly ephemeral and intermittent rivers, and strong variability in vegetation cover makes the basin a representative environment for investigating hydrosedimentological connectivity, contributing to the understanding of erosional processes and to environmental planning in semiarid basins.

Thus, considering the influence of vegetation on the hydrological and sedimentary dynamics of river basins, this study aims to evaluate how vegetation affects the connectivity and transmission of hydrosedimentological flows, with emphasis on seasonal variations in biomass in the Tigre Creek Basin, located in the semiarid region of

Paraíba, an area characterized by strong climatic seasonality and high sensitivity to erosion and sedimentation processes.

2. Study Area

The study area is in the municipality of São João do Tigre, in the Borborema mesoregion and the Western Cariri microregion of the state of Paraíba (Figure 1). The Tigre Creek Basin (RTB) covers approximately 560 km² and is entirely located within the Borborema Plateau. Elevations range from 506 m to 1,172 m, while slope values can reach 114.7% (SILVA; SOUZA, 2025).

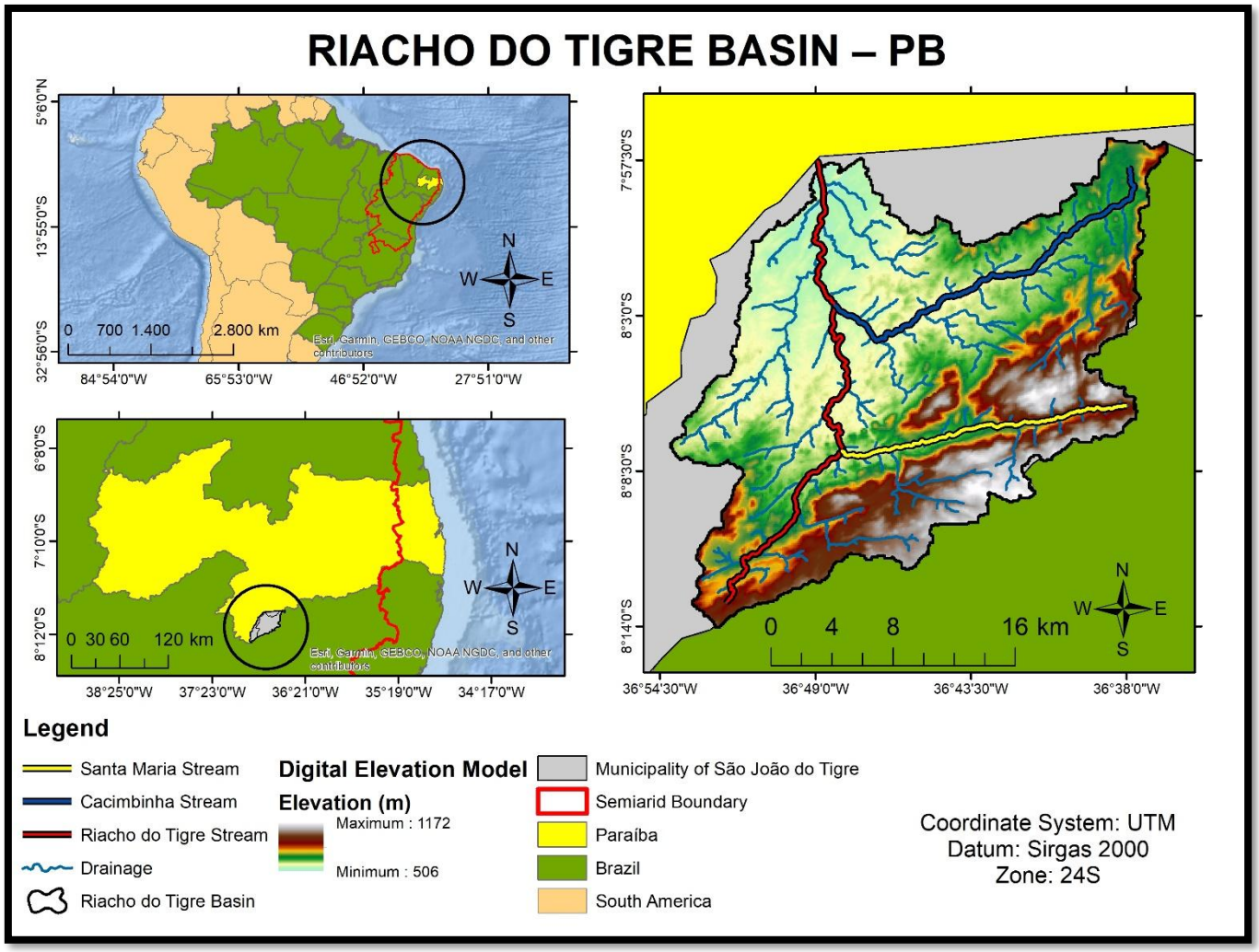


Figure 1. Location of the study area. Source: The authors.

Among the mega-geomorphological compartments of the Borborema Plateau, the municipality of São João do Tigre encompasses the Remobilized Massifs zone of the Transversal Domain, located in the higher portions, whereas the lower areas are part of the Paraíba Intraplateau Depression. The geological structure of these units, predominantly composed of crystalline rocks that are more resistant than those in adjacent formations, directly influences river and climate dynamics. While the watercourses do not cross the eastern escarpment that delimits the plateau, the local climate exhibits relief-related thermal variations, resulting in temperature differences between windward and leeward slopes (CORRÊA et al., 2010).

The predominant climate in the basin is Tropical Semiarid, with rainfall concentrated between December and April. Analysis of the historical series (1994–2023), based on data from the Executive Agency for Water Management of Paraíba (AESA) collected at the rainfall station located at an elevation of 507 m, indicates a mean annual precipitation of 423.9 mm. However, in the higher portions of the basin, rainfall tends to be greater due to orographic influence.

The rivers in the basin are predominantly ephemeral and intermittent, with no flow during most of the year and, on average, fewer than 40 days of annual flow. The main watercourses are the Tigre, Cacimbinha, and Santa Maria streams (Figure 1). The predominant biome is the Caatinga, characterized by Hyperxerophytic Caatinga and small patches of Deciduous Forest (SILVA; SOUZA, 2017). Regarding soils, four main soil classes occur in the Tigre Creek Basin: Ultisol, Entisol, Planosol, and Luvisol (SILVA; SOUZA, 2020).

Figure 2 presents the mean monthly precipitation regime at the São João do Tigre (PB) rainfall station, calculated from the 1994–2023 historical series, highlighting the strong seasonality of rainfall in the study area. The Tigre Creek Basin does not have streamflow-gauging stations with historical discharge records; therefore, the characterization of the hydrological regime was based on the historical precipitation series and the ephemeral and intermittent nature of the basin's channels.

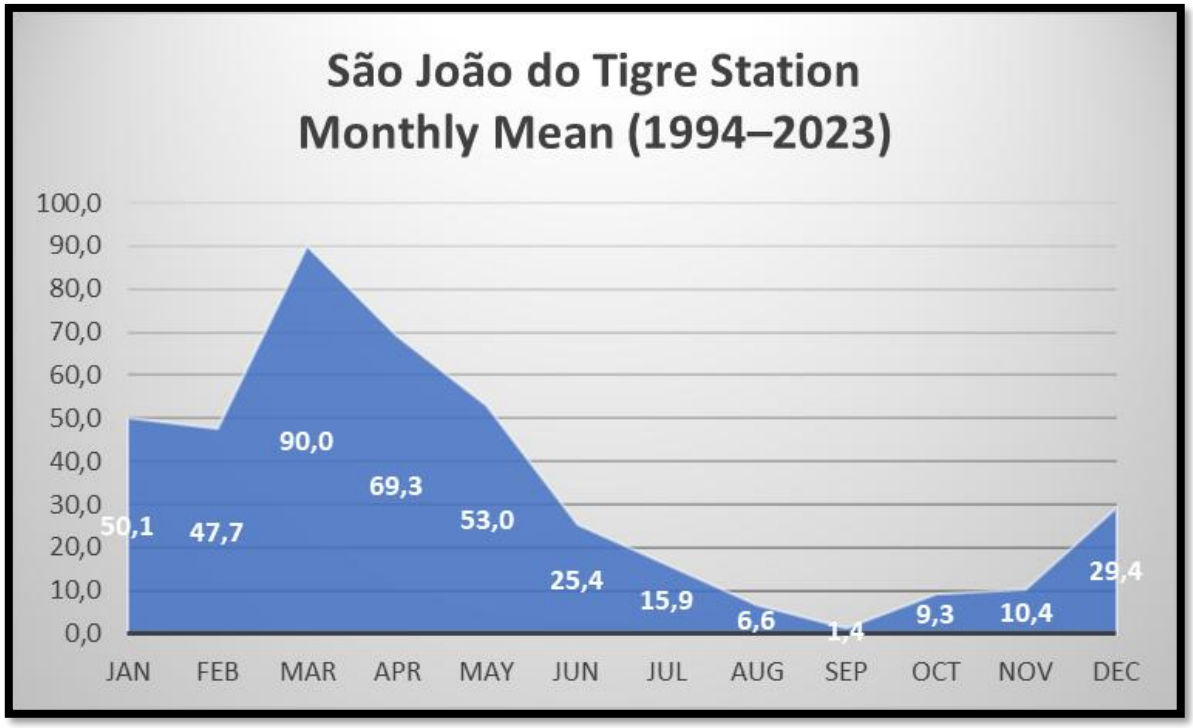


Figure 2. Mean monthly precipitation regime (mm) at the São João do Tigre (PB) rainfall station, calculated from the 1994–2023 historical series. Source: The authors.

2. Materials and Methods

The connectivity analysis at the basin scale followed the steps described in the flowchart below (Figure 3):

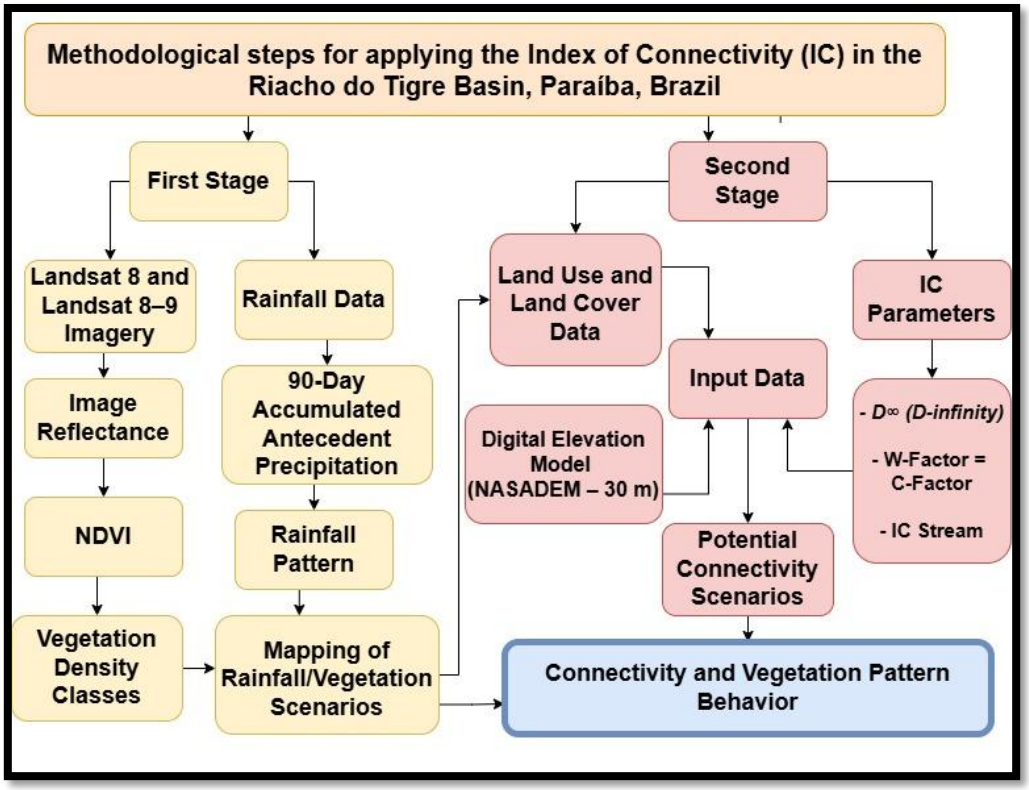


Figure 3. Flowchart of the procedures for applying the Index of Connectivity (IC) in the Tigre Creek Basin, Paraíba, Brazil. Source: The authors.

Thus, fifty-one Landsat images acquired between 2014 and 2023 were selected, considering only images with low cloud cover (less than 5% of the total area). Landsat 8 images correspond to the period from 2014 to 2021, whereas Landsat 8-9 images correspond to 2022 and 2023.

2.1. Multitemporal Analysis of Vegetation Using NDVI

Considering the basin as a whole, a temporal assessment of vegetation seasonality and, consequently, of land use and land cover was conducted. This assessment involved creating different vegetation scenarios based on the relationship between rainfall patterns and natural biomass variability, and identifying the effects of these scenarios on connectivity during rainfall events. This step is crucial for understanding how biomass density changes over time and seasonally, how these changes alter connectivity, and the relationships between these changes and rainfall characteristics.

The procedures consisted of obtaining daily rainfall data and Landsat images for the study area. Precipitation data from 1994 to 2023 were analyzed, obtained from five meteorological stations located within or around the Tigre Creek Basin: São João do Tigre, São Sebastião do Umbuzeiro, and Camalaú (Executive Agency for Water Management of the State of Paraíba – AESA), as well as Poção and Jataúba (Pernambuco Water and Climate Agency – APAC). The data were used to calculate 90- and 120-day Antecedent Cumulative Rainfall (ACR), obtained by summing the precipitation accumulated prior to the acquisition date of each Landsat image. Subsequently, ACR values were spatially interpolated using the Interpolation (IDW) tool in ArcGIS 10.5. The mean NDVI values for each Landsat image were regressed against the mean 90- and 120-day ACR values to identify the antecedent precipitation interval that best represents vegetation response. The coefficient of determination (R^2) was used to assess the fit of the established relationships.

The daily rainfall data were previously organized and inspected for consistency and gaps to ensure accurate calculation of Antecedent Cumulative Rainfall (ACR). ACR values were calculated analytically for each station and

each Landsat image acquisition date. Only the Poção (PE) station presented missing records between 2008 and 2013. For these dates, the missing records were retained as null values (Null), without artificially filling the time series, allowing spatial interpolation using the IDW method to be performed exclusively with stations that had valid data for the respective date.

Thus, satellite images with a spatial resolution of 30 m were obtained from the United States Geological Survey (USGS): Landsat 8 images from dry and rainy periods between 2016 and 2021, as well as Landsat 8-9 images from 2022 and 2023, in order to characterize the rainfall patterns affecting the basin. The period selected for image acquisition coincides with the effects of the drought that affected the Brazilian semiarid region between 2012 and 2017, which strongly impacted agricultural activities in the region (SANTANA; SANTOS, 2020), as well as with recent land-use changes following these prolonged drought periods.

Next, the Normalized Difference Vegetation Index (NDVI) was calculated from bands 5 (Near Infrared – NIR) and 4 (Red) of the Landsat 8 and Landsat 8-9 images, using the NDVI tool in the Image Analysis window of ArcGIS 10.5. NDVI allows vegetation dynamics to be identified through differences in reflectance between the red and near-infrared bands (HUANG et al., 2021), and was calculated according to Equation 1:

$$NDVI = \frac{NIR - Red}{NIR + Red} \quad (1)$$

NDVI is derived from the relationship between reflectance levels in the red and near-infrared bands of satellite images. The index is based on the fact that vegetation exhibits high reflectance in the near-infrared (NIR) bands and low reflectance in the red bands. These bands are directly related to vegetation biophysical parameters and can provide advantages such as assessing vegetation density and identifying environmental or anthropogenic changes in a river basin (DE LUCENA; PIRES; FILGUEIRA, 2017; COSTA; NUNES; AMPATZIDIS, 2020).

The mean NDVI values for each image were related to the 90- and 120-day ACR values using simple linear regression, and scatter plots were generated in Microsoft Excel. Model fit was assessed using the coefficient of determination (R^2), and the period that best fit the relationship between precipitation and vegetation response was selected. Thus, 90-day ACR was selected because it showed a stronger correlation with NDVI variation, enabling analysis of the relationships between vegetation and precipitation characteristics in the Tigre Creek Basin.

The NDVI results were grouped by the mean NDVI of each image, forming vegetation scenario groups classified as low, medium, or high biomass density, characteristic of each vegetation type. Class thresholds were defined based on standard NDVI classifications indicating the correspondence between NDVI variation and biomass, adapted from Souza and Hooke (2021), namely: very low vegetation density (0.00–0.19), low (0.19–0.35), medium (0.26–0.35), high (0.35–0.60), and very high (above 0.60). Thus, based on the relationships between rainfall patterns and NDVI, it was possible to define the seasonality of vegetation scenarios over time, determine biomass density under rainfall events, and apply these results to connectivity analyses.

2.2. Index of Connectivity

Following the definition of vegetation scenarios associated with rainfall patterns, the Index of Connectivity (IC) was applied to determine the connectivity scenarios (Figure 3). Based on topographic data from NASADEM (30 m), terrain information, such as slope, elevation, drainage density, longitudinal basin profile, and valley width, was processed to create the IC map. The IC allows the analysis of water and sediment flow transmission within a river basin, as well as the identification of natural or anthropogenic impediments that may alter flow dynamics (FRANCO; SOUZA, 2019; HOOKE; SOUZA; MARCHAMALO, 2021). The IC represents potential sediment connectivity based on the different characteristics of landscape compartments, derived from geomorphological and land-use and land-cover data (ZANANDREA et al., 2020).

The methodology used to apply the IC is based on the formulas proposed by Borselli, Cassi and Torri (2008), and subsequently adopted by Cavalli et al. (2013), Souza, Correa, and Brierley (2016), Schopper et al. (2019), Cavalli, Vericat, and Pereira (2019), Franco and Souza (2019), Souza and Hooke (2021), among others. Accordingly, this study applied the IC to the Tigre Creek Basin, incorporating the D-infinity algorithm, which allows flow direction to be calculated in areas with divergent flow. The methodology was structured to calculate the IC considering two possible depositional targets—streams and basin outlets—as proposed by Souza and Hooke (2021). However, in this study, the analysis was restricted to the IC targeting streams (IC Stream).

Equation 2 defines the Index of Connectivity (IC). In this equation, Dup (upslope) represents the contributing areas responsible for sediment production, while Ddn (downslope) represents the sediment transfer pathways, considering both surface roughness and slope gradient:

$$IC = log_{10}\left(\frac{D_{up}}{D_{dn}}\right) \quad (2)$$

The Dup (upslope) value is calculated from the variables W (mean weighting factor of the upslope contributing area), S (mean slope of this area), and A, which represents the upslope contributing area of the cell, that is, the area potentially responsible for sediment generation and supply. The term √A is used to reduce the influence of large areas and maintain the balance at the logarithmic scale of the index.

The calculation of Ddn (downslope) considers the cells located downslope, in which W represents the weighting factor associated with terrain roughness (dimensionless value of the i-th cell), and S is the slope of the same cell. Both variables are used to estimate the resistance to sediment transfer toward the drainage channel.

$$\frac{D_{up} = \overline{w}\overline{s}\sqrt{A}}{D_{dn} = \Sigma_i \frac{d_i}{w_i s_i}} \quad (3)$$

In the present study, the W parameter was represented by the C-factor of the USLE/RUSLE (Universal Soil Loss Equation / Revised Universal Soil Loss Equation), which is used to assess the effect of land use and land cover on erosion susceptibility. This factor allows areas with greater or lower soil protection to be identified based on land-use classification.

In this study, the C-factor was defined based on the NDVI (Normalized Difference Vegetation Index) responses, as presented in Table 1, and was applied to both the calculation of Dup (upslope) and Ddn (downslope), according to the formulation proposed by Borselli, Cassi, and Torri (2008). After defining the variables, the Index of Connectivity (IC) map was generated using the Raster Calculator tool in ArcGIS 10.5.

Table 1. NDVI classes, vegetation with similar NDVI responses, and C-factor assigned to each class. Adapted from Souza and Hooke (2021).

NDVI Classes	Similar NDVI Responses	C-Factor
< 0,19	Very Low	0.5
0,19-0,26	Low	0.11
0,26-0,35	Medium	0.04
0,35-0,6	High	0.0167
> 0,6	Very High	0.0004

3. Results

Upon completion of the first stage of the analysis (Figure 3), Table 2 was prepared, relating precipitation values and vegetation indices to their respective images and acquisition dates. This correlation enabled us to understand how hydrosedimentological connectivity responds to variations in rainfall and vegetation cover in the Tigre Creek Basin.

Table 2 was classified by mean NDVI for each image, with the lowest values at the bottom and the highest at the top. The vegetation scenarios were classified by mean NDVI: the lower the vegetation density, the darker the representation of the scenarios in the table, ranging from dark gray (very low density) to white (high density).

The 90- and 120-day Antecedent Cumulated Rainfall (ACR) values accompany each image (Table 2). Linear regression between the mean NDVI and ACR values indicated a better fit for the 90-day period (R^2 = 0.9869) than for the 120-day period (R^2 = 0.5562). Therefore, the 90-day ACR was adopted for the subsequent analyses (Figure 4). The highest mean NDVI value was observed in the image acquired on April 10, 2023, with a mean of 0.378 and

a maximum value of 0.617. In contrast, the lowest mean value was recorded in the image acquired on December 2, 2016, with a mean of 0.134, a maximum value of 0.426, and only 0.3 mm of 90-day ACR.

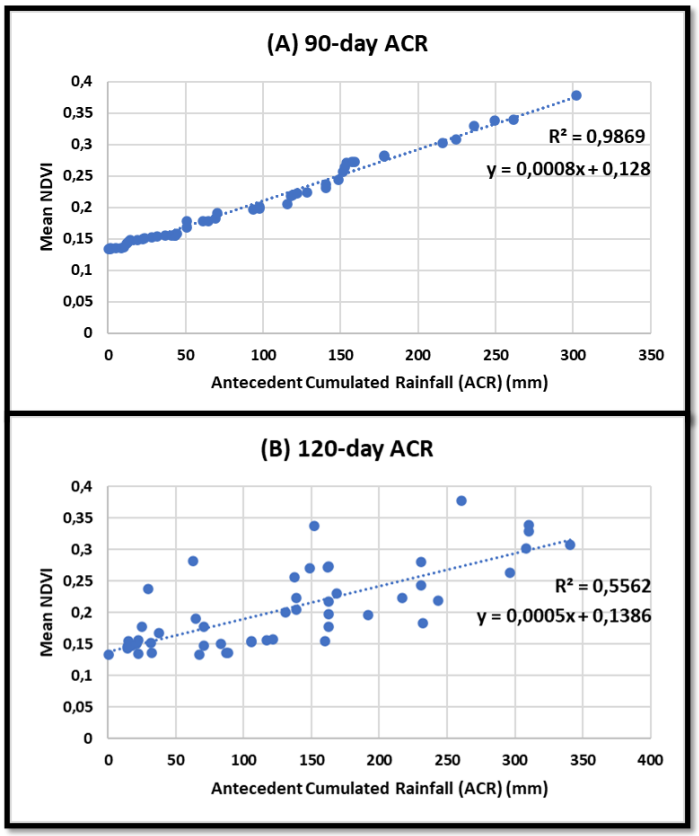


Figure 4. Relationship between mean NDVI and Antecedent Cumulated Rainfall (ACR): (A) 90-day ACR; (B) 120-day ACR. Source: The authors.

Table 2. NDVI and Antecedent Cumulative Rainfall (ACR) values corresponding to the acquisition dates of Landsat images between 2014 and 2023. Source: The authors.

Image date	90-day ACR (mm)	120-day ACR (mm)	Max. NDVI	Mean NDVI	Scenario (NDVI)
2023-04-10	249,2	260,6	0,617	0,378	High Density
2022-04-07	236,0	310,3	0,572	0,339	Medium Density
2023-01-04	151,3	151,7	0,580	0,338	
2018-04-28	302,1	310,0	0,603	0,329	
2018-05-14	224,2	340,9	0,618	0,308	
2023-05-29	261,5	307,9	0,531	0,302	
2022-01-25	61,4	62,5	0,526	0,282	
2015-05-06	178,2	231,0	0,560	0,281	
2014-06-01	140,3	162,8	0,581	0,273	
2023-01-28	157,3	161,7	0,574	0,272	
2022-12-27	148,4	148,9	0,520	0,271	
2019-06-02	152,8	296,4	0,587	0,264	
2019-02-26	128,6	137,6	0,526	0,256	Low Density

Image date	90-day ACR (mm)	120-day ACR (mm)	Max. NDVI	Mean NDVI	Scenario (NDVI)
2015-05-22	178,2	231,0	0,568	0,244	
2020-12-29	28,0	29,3	0,570	0,237	
2017-06-12	153,6	168,7	0,611	0,231	
2015-04-04	215,8	217,2	0,535	0,224	
2023-07-15	240,3	397,4	0,564	0,223	
2020-08-07	97,8	138,6	0,591	0,223	
2015-07-09	118,1	243,5	0,551	0,219	
2014-06-20	140,3	162,8	0,533	0,218	
2020-08-23	97,8	138,6	0,546	0,205	
2015-08-10	115,7	130,9	0,582	0,201	
2018-07-01	51,0	162,6	0,546	0,198	
2019-08-21	119,0	191,6	0,559	0,196	
2015-01-14	64,5	64,5	0,515	0,191	
2017-08-15	159,0	231,9	0,616	0,183	Very Low Density
2020-10-10	8,2	24,7	0,575	0,178	
2019-01-25	69,0	70,4	0,505	0,178	
2018-07-17	51,0	162,6	0,551	0,178	
2017-03-24	37,0	37,4	0,504	0,168	
2016-01-01	121,9	121,9	0,498	0,158	
2015-09-27	70,6	117,1	0,546	0,157	
2018-09-03	13,3	22,6	0,541	0,156	
2019-10-08	43,5	105,4	0,548	0,155	
2018-10-21	11,7	15,0	0,495	0,155	
2016-06-26	93,8	159,9	0,521	0,155	
2019-10-24	43,5	105,4	0,533	0,154	
2018-12-08	23,5	31,9	0,522	0,152	
2021-10-13	44,2	83,3	0,590	0,151	
2018-11-22	18,7	20,8	0,548	0,150	
2021-11-30	10,1	18,0	0,477	0,148	
2015-10-29	14,1	70,6	0,489	0,148	
2015-11-14	1,4	14,1	0,477	0,146	
2015-11-30	1,4	14,1	0,492	0,143	
2016-09-29	5,1	32,1	0,426	0,137	
2022-11-01	40,9	87,3	0,480	0,136	
2016-08-12	31,7	88,3	0,469	0,136	
2017-02-04	22,4	22,4	0,455	0,135	
2017-12-05	43,3	67,1	0,533	0,134	
2016-12-02	0,3	0,8	0,426	0,134	

The NDVI images were grouped according to the previously defined vegetation scenarios using the Mosaic to New Raster tool in ArcGIS 10.5, which allowed the generation of a representative image for each scenario (Figure 5).

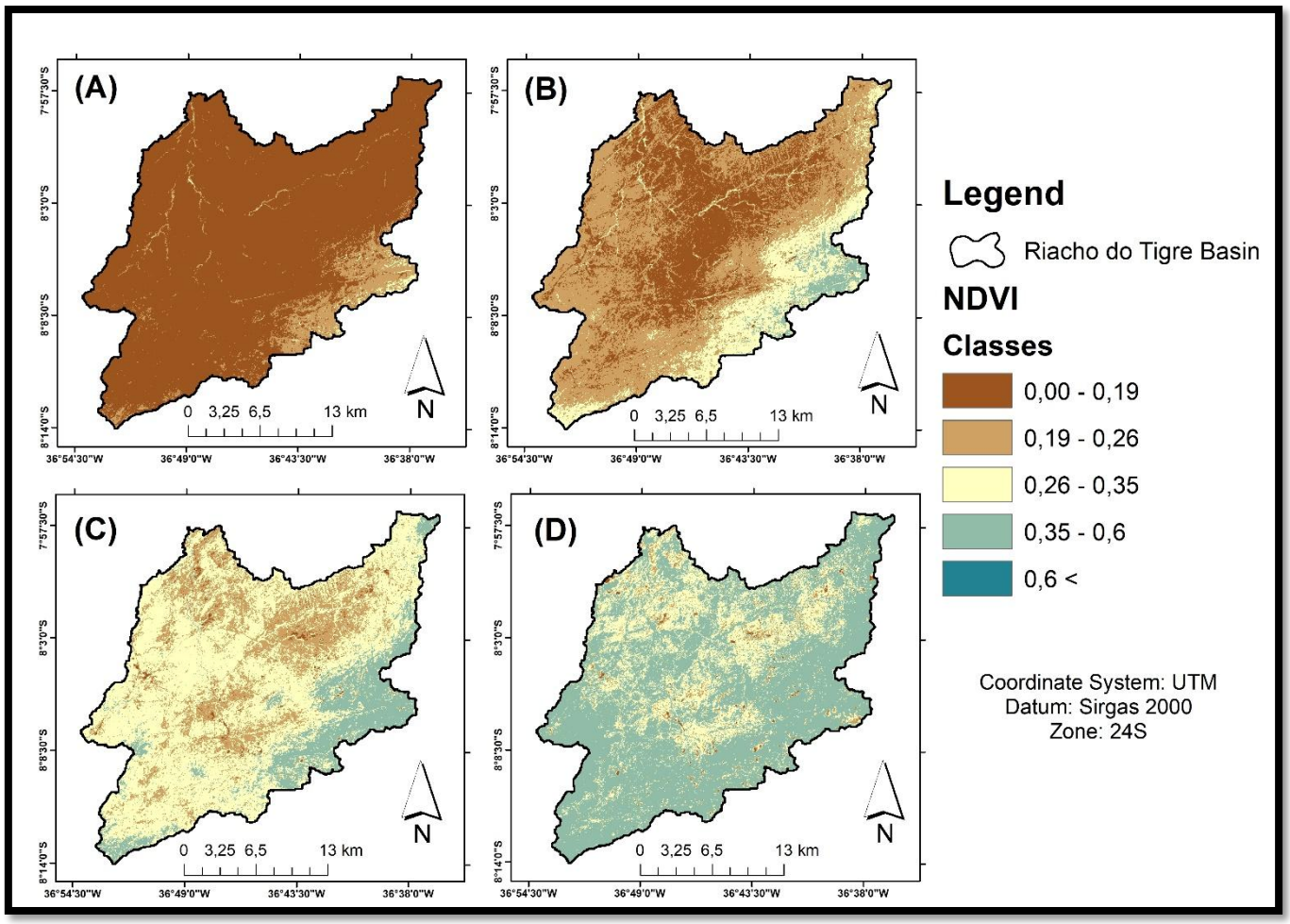


Figure 5. Vegetation maps for four scenarios according to the NDVI classes/means and vegetation cover density classification: (A) very low density (0.00–0.19); (B) low density (0.19–0.26); (C) medium density (0.26–0.35); and (D) high density (0.35–0.60). Source: The authors.

The wet scenario (D) in Figure 5 consisted solely of the image acquired on April 10, 2023, the only image with a mean NDVI value above 0.35 (Table 2) and was associated with one of the 9 highest 90-day Antecedent Cumulative Rainfall (ACR) values in the series.

The Landsat images used in this study (Table 2) were grouped into four vegetation scenarios (very dry, dry, medium, and wet) based on the NDVI intervals proposed by Souza and Hooke (2021). Additionally, Table 3 presents the mean NDVI values associated with the 90-day Antecedent Cumulated Rainfall (ACR) ranges defined by the same authors: very dry (ACR < 20 mm), dry (ACR between 20 and 59 mm), medium (ACR between 60 and 249 mm), and wet (ACR ≥ 250 mm). In addition, the mean and standard deviation of ACR are presented for each range, allowing the correspondence between vegetation response and water availability conditions to be assessed.

Table 3. NDVI classes and vegetation density of the analysed scenarios, with their respective 90-day Antecedent Cumulated Rainfall (ACR) values. Source: The authors.

	ACR < 20 mm	**20 – 59 (mm)**	**60 – 249 (mm)**	**ACR ≥ 250 mm**
	Very Dry Scenario	Dry Scenario	Medium Scenario	Wet Scenario
General Characteristics				
Mean – ACR (mm) – 90 days	8,4	38,3	140,1	281,8
Standard deviation – ACR (mm) – 90 days	6,2	9,8	51,9	28,7
ACR (mm) – 90 days (%)	20%	24%	52%	4%
NDVI: Characteristics				
Mean NDVI	0,154	0,220	0,297	0,378
Maximum NDVI	0,443	0,480	0,502	0,617
Standard Deviation of NDVI	0,028	0,052	0,051	0,065
NDVI Classes: Area Density (%) – 2014-06 to 2023-08				
0,00 – 0,19 (very low)	42%	39%	37%	30%
0,19 - 0,26 (low)	16%	15%	14%	12%
0,26 - 0,35 (medium)	20%	18%	18%	14%
0,35 - 0,6 (high)	22%	28%	31%	41%
> 0,6 (very high)	0%	0%	0%	3%

Thus, Table 3 shows that, under a very dry scenario, ACR averages 8.4 mm and the mean NDVI is 0.154 (very low density), whereas under a wet scenario, ACR averages 281.8 mm and the mean NDVI is 0.378 (high density).

The natural dynamics of vegetation across the four scenarios are presented in Figure 6, which brings together the mean NDVI values from Landsat images classified for each scenario, along with a representative image and its respective Antecedent Cumulative Rainfall (ACR) values. In general, the ACR values associated with the representative images are consistent with the rainfall conditions observed in each scenario. However, in the dry scenario, the selected image shows an ACR of 64.4 mm, which is higher than the mean for the respective rainfall range (38.3 mm), because the representative image was selected based on NDVI behaviour rather than exclusively on ACR ranges.

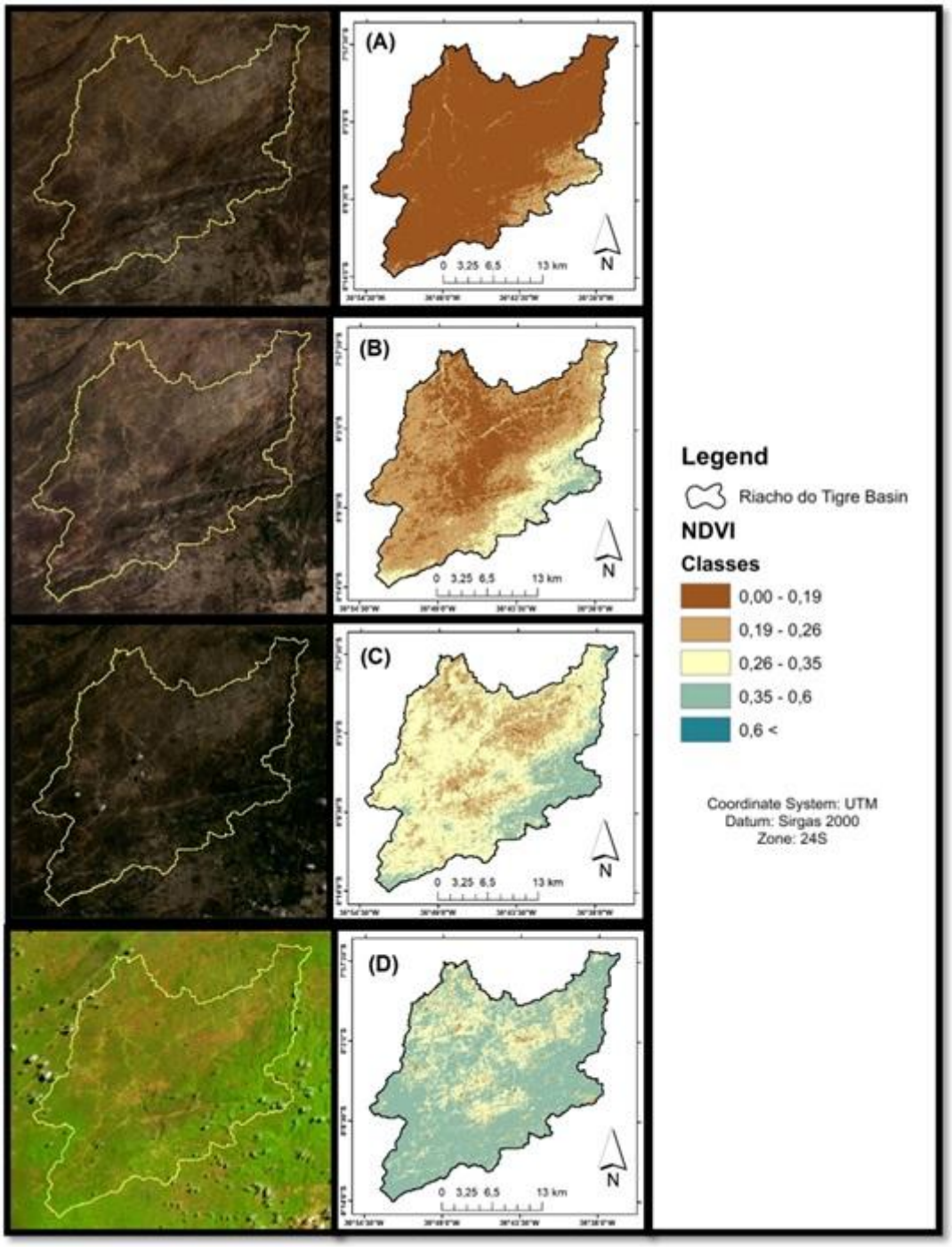


Figure 6. Natural vegetation dynamics across the four scenarios identified by NDVI and their respective 90-day Antecedent Cumulative Rainfall (ACR) conditions. For each scenario, a representative Landsat multispectral image and the corresponding mean NDVI map, derived from the set of images for that scenario, are presented. In the wet scenario, the NDVI map corresponds to the only available image. The representative images correspond to the following dates and ACR values: (A) very dry scenario (2016-12-02; ACR = 0.3 mm); (B) dry scenario (2015-01-14; ACR = 64.4 mm); (C) medium scenario (2015-05-06; ACR = 178.8 mm); and (D) wet scenario (2023-04-10; ACR = 249.2 mm). Source: The authors.

After reclassifying the NDVI results from the four scenarios into the C-factor (Table 1), the Index of Connectivity (IC stream) was applied using the C-factor and the digital elevation model of the Tigre Creek Basin as input data. Thus, the IC was applied to the four vegetation scenarios (very low density, low density, medium density, and high density), with connectivity classes ranging from very low to very high. Overall, across all scenarios, connectivity values ranged from −8.724 (minimum, very low connectivity) to 1.450 (maximum, very high connectivity).

Table 4 presents the minimum, maximum, mean, and standard deviation IC values obtained for each vegetation scenario. The results indicate higher connectivity during the driest period and lower connectivity during the wettest period. In the very dry scenario, the mean IC value is −5.377, and the maximum value is 1.450, indicating the highest connectivity among the four scenarios. In contrast, in the wet scenario, the mean IC value is −6.649, indicating the lowest connectivity among the four scenarios. The mean IC values for the dry and medium scenarios follow the same pattern: the wetter the area, the lower the connectivity.

Table 4. Potential Index of Connectivity values (minimum, maximum, mean, and standard deviation) for the four vegetation scenarios. Source: The authors.

Potential Index of Connectivity (scenarios)	Minimum	Maximum	Mean	Standard Deviation
Very Dry	-8,147	1,450	-5,377	0,731
Dry	-8,708	0,467	-5,836	0,782
Medium	-8,724	-0,556	-6,355	0,701
Wet	-8,724	-0,282	-6,649	0,696

The observed standard deviations indicate the variability in Antecedent Cumulated Rainfall (ACR) values within each rainfall range (Table 4). The lower values recorded in the very dry and dry scenarios indicate greater homogeneity in precipitation conditions, whereas the higher standard deviation in the medium scenario reflects the greater range of rainfall events encompassed by this class.

The IC maps generated for each scenario clearly show the spatial and temporal variability of connectivity in the Tigre Creek Basin and the control exerted by vegetation on connectivity (Figure 7). Connectivity increases as biomass density decreases, potentially resulting in different hydrological responses. The maps indicate that, across the four scenarios, very high and high connectivity predominate in the very dry and dry scenarios, respectively, followed by moderate connectivity in the medium scenario, and finally low and very low connectivity in the wet scenario.

Connectivity was also higher around the basin outlet and in areas with greater slope (Figure 7). At the outlet, the high connectivity values result from the high-water accumulation received by this area, as it is the point where flows from different parts of the basin converge. Degradation at the outlet of the Tigre Creek Basin—particularly that resulting from anthropogenic activities that lead to vegetation removal—may also be a factor influencing the high connectivity values.

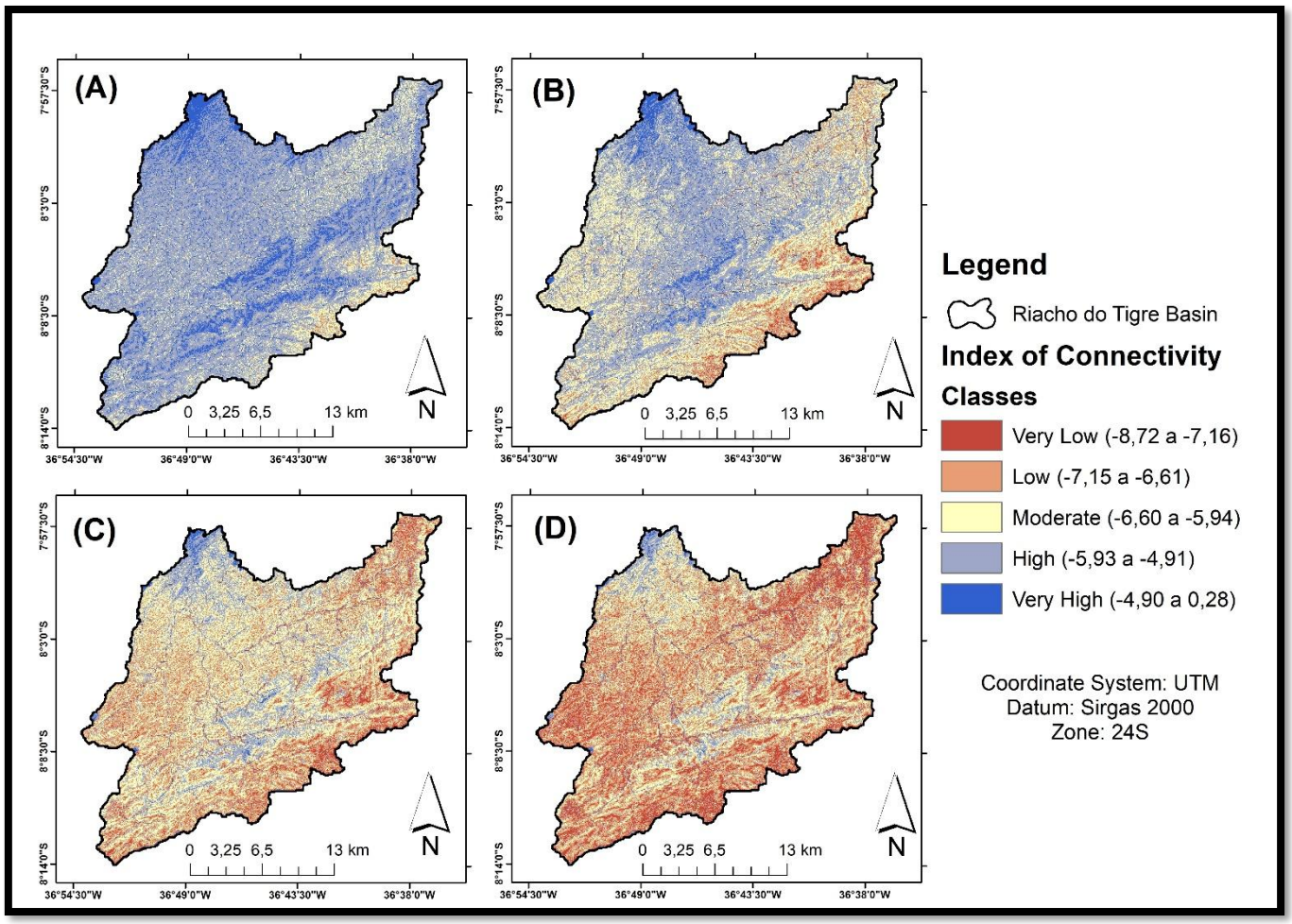


Figure 7. Connectivity Index classification maps for the four vegetation scenarios: (A) very dry; (B) dry; (C) medium; and (D) wet. Source: The authors.

In escarpment areas, steeper slopes may increase the velocity and energy of surface runoff, thereby accelerating the transfer of water and sediment along hillslopes. However, connectivity is not determined exclusively by topography but arises from interactions among relief, vegetation cover, infiltration, and the configuration of flow pathways. In this regard, Fryirs (2013) highlights that sediment transfer throughout a basin is conditioned by the existence of connections and disconnections within the system, such that source areas do not necessarily have a continuous connection with drainage channels. In a semiarid environment, Mayor et al. (2008) demonstrated that runoff connectivity is jointly controlled by topography and vegetation patterns, whereas Reaney et al. (2014) showed the combined influence of slope, infiltration, and vegetation on the generation and connectivity of surface runoff. Thus, the higher connectivity values observed in areas with steeper slopes should be interpreted together with vegetation cover and other surface characteristics that control runoff continuity (Figure 7). High connectivity predominates over 66.6% of the basin area under the very dry scenario. In the dry scenario, 45% of the area exhibits high connectivity and 31.8% exhibits moderate connectivity, making these the predominant classes. In the medium scenario, moderate connectivity predominates (43.6% of the area), followed by low connectivity (28.9%). In the wet scenario, low connectivity (38% of the area) and moderate connectivity (29.3% of the area) predominate. The very low connectivity class also reaches its greatest spatial extent in this scenario, occupying 20.1% of the area, more than twice the area recorded in the medium scenario (Table 5). Overall, there is a progressive reduction in the high and very high connectivity classes and an increase in the low and very low classes as vegetation cover becomes denser, from the very dry to the wet scenario.

Table 5. Connectivity classes distributed (%) for each vegetation scenario. Source: The authors.

Connectivity Classes (scenarios)	Very Low	Low	Moderate	High	Very High
Very Dry	0,1%	1,4%	13,7%	66,6%	18,2%
Dry	2,2%	11,1%	31,8%	45%	9,9%
Medium	7,6%	28,9%	41,6%	18%	3,9%
Wet	20,1%	38%	29,3%	9,9%	2,7%

Table 6 shows the pattern of the number of daily rainfall events at different event magnitudes, based on data from three stations covering the period from 1994 to 2023:

Table 6. Number of daily rainfall events (mm) for all months of the year, based on data from 1994–2023 from the rain gauge stations in the municipalities of São João do Tigre (PB), Poção (PE), and Camalaú (PB). Source: The authors. *No data are available for the Poção station between 2008 and 2013.*

São João do Tigre	Sep	Oct	Nov	Dec	Jan	Feb	Mar	Apr	May	Jun	Jul	Aug
Rainy Days (mm)	Number of Daily Rainfall Events											
0,1 – 9,9	9	16	15	32	56	79	106	122	112	64	63	27
10 – 24,9	1	3	2	17	31	32	34	38	28	14	12	5
25 – 49,9	0	2	5	7	13	13	25	15	11	5	2	1
> 50	0	1	1	4	4	1	11	5	3	1	0	0
Poção*	**Sep**	**Oct**	**Nov**	**Dec**	**Jan**	**Feb**	**Mar**	**Apr**	**May**	**Jun**	**Jul**	**Aug**
Rainy Days (mm)	Number of Daily Rainfall Events											
0,1 – 9,9	51	13	23	22	51	50	71	79	127	160	175	109
10 – 24,9	8	6	38	11	29	35	43	36	44	64	58	19
25 – 49,9	0	2	16	3	11	13	20	27	15	20	7	5
> 50	0	1	3	5	3	3	14	4	2	1	1	0
Camalaú	**Sep**	**Oct**	**Nov**	**Dec**	**Jan**	**Feb**	**Mar**	**Apr**	**May**	**Jun**	**Jul**	**Aug**
Rainy Days (mm)	Number of Daily Rainfall Events											
0,1 – 9,9	10	12	12	19	55	54	80	85	91	75	83	31
10 – 24,9	0	1	0	8	23	32	53	34	30	16	14	3
25 – 49,9	0	3	3	5	10	11	24	15	10	9	1	1
> 50	0	1	0	2	4	7	12	8	8	1	1	0

*No data are available for the Poção station between 2008 and 2013.

In general, March and April have the most daily precipitation events and the most events exceeding 50 mm (Table 6). According to Table 3, vegetation scenarios with medium and high densities predominate in April, suggesting that connectivity tends to be lower during this month, consistent with the patterns identified in this study.

On the other hand, September, October, and November have the fewest daily precipitation events, particularly September, which recorded no events with precipitation exceeding 25 mm (Table 6). The NDVI values for the images from September, October, and November correspond to the very low- and low-density classes (Table 2). Therefore, since September, October, and November fall within the very dry or dry vegetation scenarios, there is a tendency toward higher structural connectivity during these months, as shown by the Index of Connectivity map (Figure 7) and Table 5.

4. Discussion

The results obtained in this study demonstrate that the seasonal dynamics of vegetation play a fundamental role in modulating hydro-sedimentological connectivity in the Tigre Creek Basin. The increase in vegetation biomass was associated with a progressive reduction in the high- and very-high connectivity classes and an increase in the low- and very-low connectivity classes, indicating a lower potential for water and sediment transfer between hillslopes and the drainage network. This behaviour is related to vegetation cover's capacity to increase surface roughness, promote infiltration, and reduce surface runoff, thereby limiting connectivity between source areas and drainage channels.

The relationship between antecedent cumulated rainfall and vegetation response also reinforces the dynamic nature of hydro-sedimentological connectivity in the basin. The image acquired on 2016-12-02 presented the lowest mean NDVI value, coinciding with the period of extreme drought recorded between 2012 and 2017 in the Brazilian semiarid region (Nunes and Medeiros, 2020). This behaviour is consistent with the characteristic phenology of the Caatinga, in which seasonal leaf loss is an adaptive strategy to water deficits, while leaf renewal occurs rapidly after rainfall returns (Rufino et al., 2020). Thus, the reduction in biomass observed during dry periods does not necessarily represent vegetation mortality, but rather a physiological response to climatic conditions, with implications for hydro-sedimentological connectivity.

Another relevant aspect is that the only image from the wet scenario had an ACR of 249.2 mm, a value very close to the 250 mm threshold proposed by Souza and Hooke (2021). This result suggests that vegetation response to water availability is a continuous process and is not necessarily conditioned by rigid precipitation thresholds. Therefore, the intervals used to classify the scenarios should be understood as methodological references representing general trends in vegetation behaviour, rather than abrupt transitions between different environmental states.

The observed relationship between vegetation and connectivity is consistent with results obtained in different environments. In the Tigre Creek Basin itself, Franco and Souza (2019) observed a reduction in hydro-sedimentological connectivity under conditions of greater vegetation cover, while Souza and Hooke (2021) demonstrated that seasonal vegetation variation is an important controlling factor of hydrological connectivity in a semiarid basin in Paraíba. At the international scale, Jia-nan et al. (2024) identified, in basins in northeastern China, that sediment connectivity is related to vegetation cover conditions, interacting with topographic, climatic, and land-management factors, using the C-factor of RUSLE estimated from NDVI. Similarly, Liu et al. (2025) demonstrated in an arid basin in China that reductions in vegetation cover increase hydrological connectivity and that certain vegetation-cover thresholds may trigger transitions toward higher-connectivity states. Taken together, these studies corroborate the pattern observed in the Tigre Creek Basin and indicate that vegetation's influence on connectivity interacts with other environmental characteristics of the basin.

The results are also consistent with studies conducted in arid and semiarid regions that highlight the importance of vegetation in regulating surface flows and sediment transfer (Lesschen; Schoorl; Cammeraat, 2009; Cavalli et al., 2013). However, the influence of vegetation cover on connectivity should not be interpreted in isolation, as its effects interact with topographic and hydrological characteristics that govern flow generation and continuity. In this sense, the spatial patterns of connectivity identified in this study reflect the interaction between vegetation distribution and the basin's surface characteristics, whereas the temporal analysis demonstrates that this configuration changes with water availability.

Although previous studies have demonstrated the influence of vegetation on connectivity, approaches that rely predominantly on the spatial variability of vegetation cover may not adequately capture temporal changes associated with climatic seasonality. In this regard, the present study expands these approaches by explicitly incorporating the temporal dynamics of Caatinga vegetation, relating NDVI, antecedent cumulated rainfall, and the Index of Connectivity. The results demonstrate that seasonal variation in biomass modifies the potential for

water and sediment transfer and, consequently, the basin's connectivity states. This perspective is particularly relevant in semiarid environments, where the rapid response of vegetation to variations in water availability produces significant changes in surface conditions throughout the year.

The main contribution of this study, therefore, lies in the application of the Index of Connectivity to seasonal vegetation scenarios defined using NDVI and ACR, thereby enabling a more dynamic representation of hydro-sedimentological connectivity in a semiarid basin. This approach makes it possible to identify periods of greater potential for connectivity and, consequently, greater susceptibility to erosion and sediment transport, thereby contributing to soil management and conservation strategies. However, the adopted approach does not allow the independent quantification of the relative contributions of vegetation, topography, and precipitation to the observed variations in IC. Future studies integrating these variables with observational data on discharge, sediment load, and extreme events may provide deeper insights into the mechanisms controlling hydro-sedimentological connectivity in Dryland river basins.

5. Conclusions

This study demonstrated that hydro-sedimentological connectivity in the Tigre Creek Basin is strongly controlled by the seasonal dynamics of vegetation typical of the semiarid region of Paraíba. The integration of NDVI, antecedent cumulated rainfall, and the Index of Connectivity (IC) demonstrated that biomass variation plays a decisive role in modulating water and sediment transfer, resulting in different connectivity states over time.

The results indicated that the very dry and dry scenarios, characterized by low NDVI values and reduced vegetation cover, exhibit higher structural connectivity, favouring continuity between source areas and drainage channels. In contrast, in the medium and wet scenarios, increased biomass acts as a dissipative element for runoff energy, increasing surface roughness, promoting infiltration, and reducing the potential for sediment transport. This behaviour confirms the hypothesis that vegetation acts as a key factor controlling connectivity in basins with ephemeral and intermittent rivers.

By incorporating seasonal variability in vegetation cover into the analysis of hydro-sedimentological connectivity, the present study demonstrates that the IC can represent not only spatial patterns in the landscape but also temporal changes associated with vegetation responses to water availability. Thus, hydro-sedimentological connectivity should be understood as a dynamic process, sensitive to climatic and phenological variations, rather than merely as a fixed characteristic of the landscape.

Finally, the adopted methodology proved applicable to other basins in the Brazilian semiarid region, contributing to the identification of periods and sectors that are more susceptible to erosion and sediment transport. The results reinforce the importance of maintaining vegetation cover, particularly in areas with steeper slopes and near drainage channels, as a strategy to mitigate environmental degradation and support the sustainable planning and management of fluvial systems in semiarid regions.

Author Contributions: A.F.P.L.S.: Conceptualization, Methodology, Investigation, Data Curation, Analysis, Data Processing, Writing – Original Draft, Review and Editing. J.O.P.S.: Conceptualization, Supervision, Methodology, Translation Review, Review and Editing of the manuscript.

Funding: This research received no specific funding from funding agencies, public institutions, commercial entities, or not-for-profit organizations.

Acknowledgments: The authors thank the Federal University of Paraíba (UFPB) for institutional support, support for field activities, and the provision of laboratory infrastructure used in the development of this study. The authors also thank the Study Group on Semiarid Fluvial Environments (GEAFS) for the scientific discussions and contributions.

Conflict of Interest: The authors declare no conflict of interest.

Declaration of Use of Artificial Intelligence: During the preparation of this manuscript, the authors used the ChatGPT tool (OpenAI) during the writing stage to assist in reviewing and improving the text, and during the translation stage to assist in translating the manuscript into English. All content produced or suggested by the tool was critically reviewed and validated by the authors, who assume full responsibility for the final content of the manuscript.

References

1. AESA – Agência Executiva de Gestão das Águas do Estado da Paraíba. **Pluviometria diária por posto pluviométrico entre os dias 01/01/1994 e 31/12/2023**. Disponível em: http://sic.pb.gov.br. Acesso em: 12 nov. 2023.
2. ALMEIDA, J. D. M.; CORREA, A. C. B. Conectividade da paisagem e a distribuição de plainos aluviais em ambiente semiárido. **Revista Brasileira de Geomorfologia**, 21(1), p. 171-183, 2020. DOI: 10.20502/rbg.v21i1.1663
3. APAC – Agência Pernambucana de Águas e Clima. **Dados pluviométricos diários por estação**. Disponível em: http://www.apac.pe.gov.br. Acesso em: 12 nov. 2023.
4. BLANTON, P.; MARCUS, W. A. Transportation infrastructure, river confinement, and impacts on floodplain and channel habitat, Yakima and Chehalis rivers, Washington, U.S.A. **Geomorphology**, v. 189, p. 55-65, 2013. DOI: 10.1016/j.geomorph.2013.01.016
5. BORSELLI, L.; CASSI, P.; TORRI, D. Prolegomena to sediment and flow connectivity in the landscape: A GIS and field numerical assessment. **Catena**, v. 75, n. 3, p. 268-277, 2008. DOI: 10.1016/j.catena.2008.07.006
6. BRACKEN, L. J. et al. Concepts of hydrological connectivity: Research approaches, Pathways and future agendas. **Earth-Science Reviews**, v. 119, p. 17-34, 2013. DOI: 10.1016/j.earscirev.2013.02.001
7. BRACKEN, L. J.; CROKE, J. The concept of hydrological connectivity and its contribution to understanding runoff-dominated geomorphic systems. **Hydrological Processes**, v. 21, n. 13, p. 1749-1763, 2007. DOI: 10.1002/hyp.6313
8. BRACKEN, L. J.; WAINWRIGHT, J. Equilibrium in the balance? Implications for landscape evolution from dryland environments. **Geological Society Special Publication**, v. 296, p. 29-46, 2008. DOI: 10.1144/sp296.3
9. BRIERLEY, G.; FRYIRS, K.; JAIN, V. Landscape connectivity: The geographic basis of geomorphic applications. **Area**, v. 38, n. 2, p. 165-174, 2006. DOI: 10.1111/j.1475-4762.2006.00671.x
10. CAVALLI, M. et al. Geomorphometric assessment of spatial sediment connectivity in small Alpine catchments. **Geomorphology**, v. 188, p. 31-41, 2013. DOI: 10.1016/j.geomorph.2012.05.007
11. CAVALLI, M.; VERICAT, D.; PEREIRA, P. Mapping water and sediment connectivity. **Science of the Total Environment**, v. 673, p. 763-767. 2019. DOI: 10.1016/j.scitotenv.2019.04.071
12. CORRÊA, A. C. DE B. et al. Megageomorfologia e morfoestrutura do Planalto da Borborema. **Revista do Instituto Geológico**, v. 31, n. 1–2, p. 35-52, 2010. DOI: 10.5935/0100-929X.20100003
13. COSTA, L.; NUNES, L.; AMPATZIDIS, Y. A new visible band index (vNDVI) for estimating NDVI values on RGB images utilizing genetic algorithms. **Computers and Electronics in Agriculture**, v. 172, 105334, 2020. DOI: 10.1016/j.compag.2020.105334
14. DE LUCENA, A. P.; PIRES, A. L.; FILGUEIRA, H. J. A. The NVDI use in the environmental degradation study of the Gramame river basin, Paraíba state. **Geociencias**, v. 36, n. 4, p. 755–769, 2017. https://doi.org/10.5016/geociencias.v36i4.12752
15. FARIA, A. P. Transporte De Sedimentos Em Canais Fluviais De Primeira Ordem: Respostas Geomorfológicas. **Revista Brasileira de Geomorfologia**, v. 15, n. 2, p.191-202, 2014. DOI: 10.20502/rbg.v15i2.410
16. FRANCO, V. V.; SOUZA, J. O. P. DE. Conectividade de sedimentos na Bacia Hidrográfica Tigre Creek, ambiente semiárido no município de São João do Tigre-PB. **GEOUSP Espaço e Tempo (Online)**, v. 23, n. 3, p. 697–711, 2019. DOI: 10.11606/issn.2179-0892.geousp.2019.151940
17. FRYIRS, K. (Dis)Connectivity in catchment sediment cascades: A fresh look at the sediment delivery problem. **Earth Surface Processes and Landforms**, v. 38, n. 1, p. 30-46, 2013. DOI: 10.1002/esp.3242
18. HENARES, S.; DONSELAAR, M. E.; CARACCIOLO, L. Depositional controls on sediment properties in dryland rivers: Influence on near-surface diagenesis. **Earth-Science Reviews**, v. 208, 103297, 2020. DOI: 10.1016/j.earscirev.2020.103297
19. HOOKE, J.; SOUZA, J.; MARCHAMALO, M. Evaluation of connectivity indices applied to a Mediterranean agricultural catchment. **Catena**, v. 207, 105713, 2021. DOI: 10.1016/j.catena.2021.105713
20. HUANG, S. et al. A commentary review on the use of normalized difference vegetation index (NDVI) in the era of popular remote sensing. **Journal of Forestry Research**, v. 32, p. 1–6, 2021. DOI: 10.1007/s11676-020-01155-1
21. JAMES, L. A. Ten conceptual models of large-scale legacy sedimentation – A review. **Geomorphology**, v. 317, p. 199-217, 2018. DOI: 10.1016/j.geomorph.2018.05.021
22. JIA-NAN, W.; HAO-MING, F.; YAN-FENG, J. Spatial variation characteristics and influencing factors of sediment connectivity in the black soil region of northeast China. **Geoderma**, v. 446, 116895, 2024. DOI: 10.1016/j.geoderma.2024.116895
23. LEIBOWITZ, S. G. et al. Connectivity of Streams and Wetlands to Downstream Waters: An Integrated Systems Framework. **Journal of the American Water Resources Association**, v. 54, n. 2, p. 298-322, 2018. DOI: 10.1111/1752-1688.12631

24. LESSCHEN, J. P.; SCHOORL, J. M.; CAMMERAAT, L. H. Modelling runoff and erosion for a semi-arid catchment using a multi-scale approach based on hydrological connectivity. **Geomorphology**, v. 109, n. 3–4, p. 174-183, 2009. DOI: 10.1016/j.geomorph.2009.02.030
25. LIMA, S.; FELTRIN, R. M. AVALIAÇÃO DA EVOLUÇÃO DO ASSOREAMENTO NA REGIÃO DAS MINAS DO CAMAQUÃ , MUNICÍPIO DE CAÇAPAVA DO SUL , RS. **XXV SBRH - Simpósio Brasileiro de Recursos Hídricos**, n. 55, p. 1–10, 2019.
26. LIU, X.; XUE, J.; CHANG, J.; SUN, H.; ZHAO, Y.; LI, F.; WANG, S.; LEI, Q. Hydrological connectivity-mediated spatial vegetation patterns and regime shifts in drylands. **Ecological Indicators**, v. 171, 113194, 2025. DOI: 10.1016/j.ecolind.2025.113194
27. MARCHAMALO, M.; HOOKE, J. M.; SANDERCOCK, P. J. Flow and Sediment Connectivity in Semi-arid Landscapes in SE Spain: Patterns and Controls. **Land Degradation and Development**, v. 27, n. 4, p. 1032-1044, 2016. DOI: 10.1002/ldr.2352
28. MAYOR, A. G.; BAUTISTA, S.; SMALL, E. E.; DIXON, M.; BELLOT, J. Measurement of the connectivity of runoff source areas as determined by vegetation pattern and topography: a tool for assessing potential water and soil losses in drylands. **Water Resources Research**, v. 44, W10423, 2008. DOI: 10.1029/2007WR006367.
29. MICHAELIDES, K.; MARTIN, G. J. Sediment transport by runoff on debris-mantled dryland hillslopes. **Journal of Geophysical Research: Earth Surface**, v. 117, n. 3, F03014, 2012. DOI: 10.1029/2012JF002415
30. MILAN, D. et al. Morphodynamics of bedrock-influenced dryland rivers during extreme floods: Insights from the Kruger National Park, South Africa. **Bulletin of the Geological Society of America**, v. 130, n. 11–12, p. 1825–1841, 2018. DOI: 10.1130/B31839.1
31. MORGAN, B. E. et al. Lateral and longitudinal distribution of riparian vegetation along an ephemeral river in Namibia using remote sensing techniques. **Journal of Arid Environments**, v. 181, 104220, 2020. DOI: 10.1016/j.jaridenv.2020.104220
32. NAJAFI, S. et al. Sediment connectivity concepts and approaches. **Catena**, v. 196. 104880, 2021. DOI: 10.1016/j.catena.2020.104880
33. NUNES, L.; MEDEIROS, P. Análise histórica da severidade de secas no Ceará: efeitos da aquisição de capital hidráulico sobre a sociedade. **Revista de Gestão de Água da América Latina**, v. 17, e18, 2020. DOI: 10.21168/rega.v17e18
34. PEREIRA, C. Measuring and Modeling Sediment Transport: Case Study of a Brazilian Cerrado (Savanna) River. In: SCHULZ, H.; SIMÕES, A. (Ed.) **Cutting-Edge Advances in Hydraulic Engineering**. IntechOpen, p. 1-22, 2025. DOI: 10.5772/intechopen.1011122
35. POEPPL, R. E.; KEESSTRA, S. D.; MAROULIS, J. A conceptual connectivity framework for understanding geomorphic change in human-impacted fluvial systems. **Geomorphology**, v. 277, p. 237-250, 2017. DOI: 10.1016/j.geomorph.2016.07.033
36. PRINGLE, C. What is hydrologic connectivity and why is it ecologically important? **Hydrological Processes**, v. 17, n. 13, p. 2685–2689, 2003. DOI: 10.1002/hyp.5145
37. REANEY, S. M.; BRACKEN, L. J.; KIRKBY, M. J. The importance of surface controls on overland flow connectivity in semi-arid environments: results from a numerical experimental approach. **Hydrological Processes**, v. 28, n. 4, p. 2116-2128, 2014. DOI: 10.1002/hyp.9769
38. RUFINO, M. K. G. et al. Leaf deciduousness and flowering of woody caatinga species. **Biotemas**, v. 33, n. 4, P. 1-10, 2020. 10.5007/2175-7925.2020.e72364
39. SANDERCOCK, P. J.; HOOKE, J. M.; MANT, J. M. Vegetation in dryland river channels and its interaction with fluvial processes. **Progress in Physical Geography**, v. 31, n. 2, p. 107-129, 2007. DOI: 10.1177/0309133307076106
40. SANTANA, A. S. DE; SANTOS, G. Impactos da seca de 2012-2017 na região semiárida do Nordeste: notas sobre a abordagem de dados quantitativos e conclusões qualitativas. **Boletim Regional, Urbano e Ambiental**, n. 22, p. 119–129, 2020. DOI: 10.38116/brua22
41. SCAPIN, J.; PAIVA, J.; BELING, F. Avaliação de Métodos de Cálculo do Transporte de Sedimentos em um Pequeno Rio Urbano. **Revista Brasileira de Recursos Hídricos**, n. 12, v. 4, 2007. DOI: 10.21168/rbrh.v12n4.p5-21
42. SCHOPPER, N. et al. Analysis of lateral sediment connectivity and its connection to debris flow intensity patterns at different return periods in the Fella River system in northeastern Italy. **Science of the Total Environment**, v. 658, p. 1586-1600, 2019. DOI: 10.1016/j.scitotenv.2018.12.288
43. SILVA JR, V. P. et al. Produção de água e sedimentos em bacia representativa do semiárido pernambucano. **Revista Brasileira de Engenharia Agrícola e Ambiental**, v. 15, n. 10, p.1073–1081, 2011. DOI: 10.1590/S1415-43662011001000012
44. SILVA, A. F. P. DE L.; SOUZA, J. O. P. DE. CARACTERIZAÇÃO HIDROSSEDIMENTOLÓGICA DOS TRECHOS ALUVIAIS DA BACIA TIGRE CREEK – PB. **Caminhos de Geografia**, v. 18, n. 63, p. 57–89, 2017. DOI: 10.14393/RCG186303

45. SILVA, A. F. P. DE L.; SOUZA, J. O. P. DE. GEOQUÍMICA E MINERALOGIA DOS DEPÓSITOS ALUVIAIS NA BACIA DO TIGRE CREEK, SEMIÁRIDO PARAIBANO. **GEOgraphia**, v. 22, n. 49, P. 1-15, 2020. DOI: 10.22409/GEOgraphia2020.v22i49.a40840
46. SILVA, A.; SOUZA, J. CARACTERIZAÇÃO MORFOLÓGICA E SEDIMENTOLÓGICA DOS AMBIENTES ALUVIAIS DA BACIA DO TIGRE CREEK – PB. **Revista GeoInterações**, v. 9, n. 1, p.47-61, 2025. DOI: 10.59776/2526-3889.2025.6088
47. SOUZA, J. O. P. DE; CORREA, A. C. B. Conectividade e área de captação efetiva de um sistema fluvial semiárido: bacia do riacho Mulungu, Belém de São Francisco-PE. **Sociedade & Natureza**, v. 24, n. 2, p. 319-332, 2012. Disponível em: https://seer.ufu.br/index.php/sociedadenatureza/article/view/14468. Acesso em: 19 dec. 2025.
48. SOUZA, J. O. P.; CORREA, A. C. B.; BRIERLEY, G. J. An approach to assess the impact of landscape connectivity and effective catchment area upon bedload sediment flux in Saco Creek Watershed, Semiarid Brazil. **Catena**, v. 138, p. 13-29, 2016. DOI: 10.1016/j.catena.2015.11.006
49. SOUZA, J.; HOOKE, J. Influence of seasonal vegetation dynamics on hydrological connectivity in tropical drylands. **Hydrological Processes**, v. 35, n. 11, e14427, 2021. DOI: 10.1002/hyp.14427
50. TOOTH, S. Process, form and change in dryland rivers: A review of recent research. **Earth Science Reviews**, v. 51, n. 1–4, p. 67-107, 2000. DOI: 10.1016/S0012-8252(00)00014-3
51. WOHL, E. Connectivity in rivers. **Progress in Physical Geography**, v. 41, n. 3, p. 345-362, 2017. DOI: 10.1177/03091333177149
52. ZANANDREA, F. et al. CONECTIVIDADE DOS SEDIMENTOS: CONCEITOS, PRINCÍPIOS E APLICAÇÕES. **Revista Brasileira de Geomorfologia**, v. 21, n. 2, p.435-459, 2020. DOI: 10.20502/rbg.v21i2.1754

This work is licensed with a Creative Commons Attribution 4.0 International License (http://creativecommons.org/licenses/by/4.0/) – CC BY. Esta licença permite que outros distribuam, remixem, adaptem e criem a partir do seu trabalho, mesmo para fins comerciais, desde que lhe atribuam o devido crédito pela criação original.